GaAs/InGaAs quantum well infrared photodetector with a cutoff wavelength at 35 μm

A. G. U. Perera[a)] and S. G. Matsik
Department of Physics and Astronomy, Georgia State University, Atlanta, Georgia 30303

H. C. Liu, M. Gao, and M. Buchanan
Institute for Microstructural Sciences, National Research Council, Ottawa K1A 0R6, Canada

W. J. Schaff and W. Yeo
School of Electrical Engineering, Cornell University, Ithaca, New York 14853

(Received 22 March 2000; accepted for publication 31 May 2000)

GaAs/InGaAs far-infrared quantum well photodetectors based on a bound-to-continuum intersubband transition with a (zero response) cutoff wavelength of 35 μm are reported. A peak responsivity of 0.45 A/W and detectivity of $6.0\times10^{9}\,\mathrm{cm}\sqrt{\mathrm{Hz}}/\mathrm{W}$ at a wavelength of 31 μm and a temperature of 4.2 K have been experimentally achieved. Infrared response was observed at temperatures up to 18 K. A calculated responsivity spectrum using a bound-to-continuum line shape corrected for phonon absorption is fitted to the experimental response. The calculated line shape without absorption gives a cutoff wavelength of 38 μm with a peak responsivity of 0.50 A/W and a detectivity of $6.6\times10^{9}\,\mathrm{cm}\sqrt{\mathrm{Hz}}/\mathrm{W}$ at 32 μm. *© 2000 American Institute of Physics.*
[S0003-6951(00)00931-1]

Quantum well infrared photodetectors (QWIPs) have attracted attention[1] due to their high detectivity, extremely good uniformity, radiation hardness, and low power consumption. QWIPs have already found applications at wavelengths around 10 μm[2] and have been demonstrated in AlGaAs with cutoff wavelengths out to 28 μm.[3] Extending the wavelength range of QWIPs would be important for space applications in areas such as infrared astronomy and satellite mapping, where arrays would be an advantage as an alternative to the currently available Ge detectors with detectivities ranging from 10^{9} to $10^{14}\,\mathrm{cm}\sqrt{\mathrm{Hz}}/\mathrm{W}$.[4] In this letter far-infrared results on a GaAs/InGaAs QWIP with cutoff wavelength λ_c of 35 μm are presented.

The nominal parameters of the molecular beam epitaxial (MBE) grown detector were 338 Å GaAs barriers and 83 Å $In_{0.087}Ga_{0.913}As$ wells as shown in Fig. 1. The structure consisted of 20 periods with a nominal 423 Å GaAs undoped buffer region between the contacts and the wells at each end of the multiquantum well region to form the injection barrier. The contacts were doped with Si to $1\times10^{18}\,\mathrm{cm}^{-3}$, and the wells were δ doped with Si to $4.0\times10^{10}\,\mathrm{cm}^{-2}$. Based on these parameters the ground and first excited state energies would be expected at 24 and 59.5 meV respectively. A designed barrier height of 56.5 meV leads to a bound-to-continuum transition. The QWIP peak and (zero response) cutoff wavelengths expected from these energy levels and barrier height would be 34 and 38 μm, respectively. The experimental peak was observed at 31 μm and the cutoff at 35 μm under backilluminated conditions. For wavelengths in the range 35–40 μm, there is strong restrahlen absorption in the substrate. The use of front illumination with a grating structure to couple the radiation to the QWIP[2] will reduce two phonon absorptions that are also present in this range but will not eliminate the restrahlen effects.

The GaAs/InGaAs far-infrared (FIR) QWIPs were fabricated by etching 240 μm×240 μm mesas using conventional wet chemical etching techniques. Ni/Ge/Au ohmic contacts were evaporated onto the top and bottom layers. The dark current–voltage curves measured at different temperatures as shown in Fig. 2(a) are highly symmetric, indicating negligible dopant migration in the well.[5] This is consistent with having minimal dopant migration due to the low growth temperature (~500 °C) for InGaAs. Below 25 K the dark current was dominated by tunneling and field assisted tunneling, slowly increasing with temperature. Above 25 K, the thermionic component dominated, and increased rapidly with an effective activation energy of ~18±4 meV (significantly lower than 31.5 meV between the top of the Fermi sea for the ground state and the top of the barrier based on the nominal parameters) obtained from an Arrhenius plot as shown in the inset in Fig. 2. The discrepancy is probably due

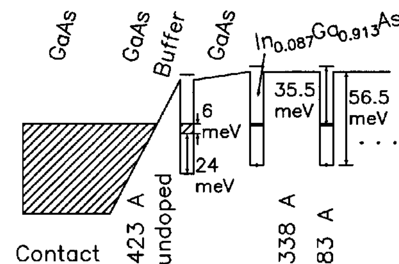

FIG. 1. Structure designed for the GaAs/InGaAs QWIP with predicted peak and cutoff wavelength of 34 and 38 μm, respectively, based on the energy levels and barrier height obtained from the nominal parameters. The 338-Å-thick barriers were GaAs and the 83 Å wells had an In fraction of 0.087 δ doped to $4\times10^{10}\,\mathrm{cm}^{-2}$ with Si. Buffer regions 423 Å thick adjacent to the first and last wells served as contact barriers and the contacts were Si doped to $1\times10^{18}\,\mathrm{cm}^{-3}$. Note the increased Fermi level in the first and second wells due to the space charge associated with band bending.

a)Electronic mail: uperera@gsu.edu

 © 2000 American Institute of Physics

Downloaded 01 Feb 2001 to 131.96.4.23. Redistribution subject to AIP copyright, see http://ojps.aip.org/aplo/aplcpyrts.html.

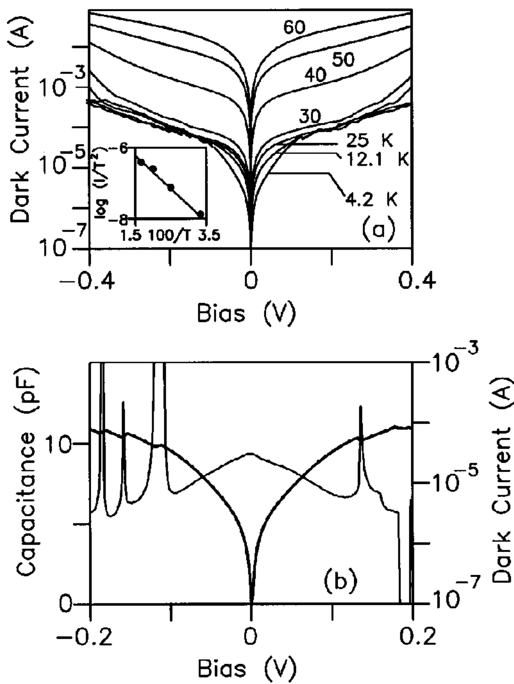

FIG. 2. (a) Dark current vs bias voltage curves at different temperatures for the FIR GaAs/InGaAs quantum well photodetector. Positive bias means top positive. The inset shows an Arrhenius plot from which the effective value of $\Delta = 18 \pm 4$ meV for injection was obtained. (b) Capacitance vs voltage (thin curve) for a frequency of 1 MHz and current vs voltage (thick curve) at 4.2 K. The spikes in capacitance correspond to the biases where negative differential conductivity is observed. Similar $C-V$ curves were obtained for frequencies above 20 kHz.

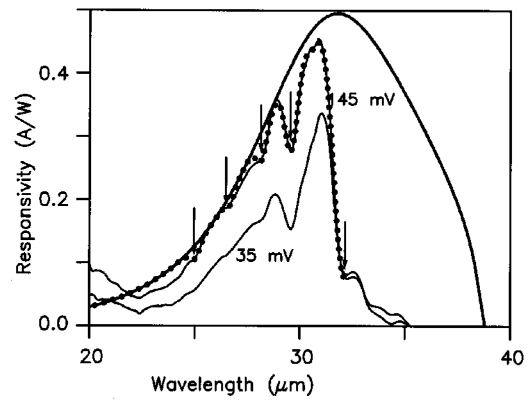

FIG. 3. Measured and calculated spectral response of GaAs/InGaAs FIR detector measured at 4.2 K under different bias values. The valleys indicated by the vertical arrows at 26.6, 28.3, 29.6, and 32.3 μm are due to two-phonon absorption of GaAs substrate (Ref. 9). The thick line shows a calculated response determined using an intersubband transition from a 24 meV ground state to a 60 meV first excited state with a barrier of 56.5 meV. The dotted curve is the theoretical response corrected for the two-phonon absorptions indicated. Note the almost exact fit to the 145 mV bias experimental response. A similar curve could be obtained for 35 mV bias.

to defects and leakage which will give a lower activation energy than expected. This is supported by the broad x-ray diffraction peaks obtained from the sample, indicating some degree of relaxation in the structure which exceeds the critical thickness.[6] Simply stated, it is believed that the device is not ideal, providing additional current paths. Also shown in Fig. 2(b) is a plot of capacitance versus bias at 1 MHz and 4.2 K for biases below 0.2 V. The capacitance for most of the region is close to the geometrical capacitance of 7 pF with several large spikes occurring at bias values where negative differential conductance is observed in the $I-V$ curve. The negative differential resistance features are not observed for thick barrier detectors operating at shorter wavelengths due to the reduction in tunneling effects. However, with the reduced barrier height of the present sample tunneling may become significant. The capacitance spikes are probably due to resonant tunneling effects in the structure as was seen previously by Liu *et al.*,[7] who observed capacitance spikes which increased in amplitude at low frequencies at the same biases as negative differential resistance. The device was modeled by representing the high and low field regions each as a capacitor and resistor in parallel. The peaks were attributed to changes in the resistance of the regions as the bias was varied. In the present case under negative bias three spikes are seen with bias differences on the same order as the difference between energy levels. The variation is probably due to contact resistance and band bending effects which will increase and decrease the bias difference between alignments, respectively. The asymmetry in the peak positions is probably due to the increased sensitivity to small variations caused by the excited state being in the continuum rather than bound as in the case for most resonant structures. The amplitude of the spikes increases with decreasing frequency reaching 150 nF for 1 kHz and 1 μF at 100 Hz. Throughout the frequency range conductance remained constant at a given bias. For low frequencies ($<10^5$ Hz) capacitive reactance is relatively constant, indicating that the processes involved may be occurring in a few microsecond time scales or faster.

The responsivity spectra of the detector were measured using a Perkin–Elmer, system 2000, Fourier transform infrared spectrometer. The detector was backilluminated through a 45° polished facet and a Si composite bolometer was used as the reference detector to obtain the background spectrum and the responsivity. Figure 3 shows responsivity spectra of the detector at 4.2 K for 35 and 145 mV bias values. The measured responsivity curves were mainly located in the range of 25–34 μm, with a measured highest responsivity of 0.45 A/W at a bias of 0.145 V. The thick line in Fig. 3 shows the calculated response for a bound-to-continuum intersubband transition for a detector with a ground state of 24 meV and a first excited state of 59.5 meV with a barrier height of 56.5 meV obtained from the nominal parameters following the model given by Choi.[8] In the model the response is assumed to have the same shape as the absorption which is given by

$$A = 2C \frac{\sqrt{E}}{1 + C^2 E (E - E_{\min})^2}, \tag{1}$$

where E is the energy of the excited electron and $E_{\min}$ is the energy of the first excited state both measured relative to the top of the barrier. The parameter C is given by

$$C = \frac{\hbar}{D^2 L} \sqrt{2/m_b^*}, \tag{2}$$

where D is a coupling constant taken as a fitting parameter, L is the length of one period of the well, and m_b^* is the effective electron mass in the barrier. The effect of changing D in the model is to vary the width of the response peak as

Downloaded 01 Feb 2001 to 131.96.4.23. Redistribution subject to AIP copyright, see http://ojps.aip.org/aplo/aplcpyrts.html.

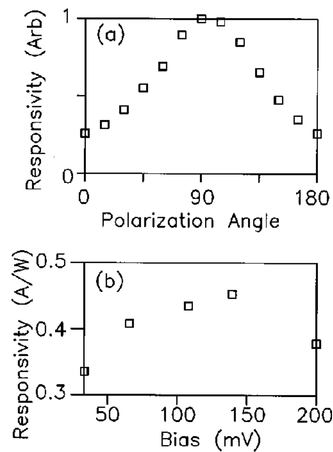

FIG. 4. (a) The dependence of responsivity on polarization for 31 μm indicating an intersubband transition. (b) The responsivity vs bias at 31 μm showing a relatively constant response with bias as is expected for a QWIP.

well as shift the peak response. The absorption equation was fit to the short wavelength region (25–29 μm) of the response to determine $D=2.3$ meV. The response without absorption is then given by $R=BA$, where B is a constant chosen to fit the measured response. The vertical arrows at 26.6, 28.3, 29.6, and 32.3 μm indicate the multiphonon absorption in the substrate.[1,9] When corrected for the multiphonon absorptions by using Gaussian absorption features centered on the multiphonon lines, the model response almost exactly matches the experimental response at 145 mV as seen by the dotted line in Fig. 3. The peak of the calculated model response without absorption occurs at 32 μm with a responsivity of 0.50 A/W. This indicates that the effect of multiphonon absorption in the substrate on the modeled response could reduce the peak response by ~10% and reduce the cutoff wavelength from 38 μm to the observed value of 35 μm. The cutoff wavelength, peak wavelength, and short wavelength regions of the observed spectra could not all be matched simultaneously without including the effects of these absorption lines. Well widths in the range 83 ± 5 Å and In fractions in the range 0.087 ± 0.005 produced peak and cutoff wavelengths that agreed with the experimental data within 1 μm. Increasing the In fraction and narrowing the wells decreased the response wavelength significantly while the opposite changes increased the response wavelengths. Adjusting the device parameters used in the model to reduce the activation energy to 22 meV (the maximum from the Arrhenius plot) produced model spectra with peak and cutoff wavelengths much longer than the experimental results. Above 32.6 μm there is a strong absorption region[9] which blocks the incident radiation. The shorter wavelength absorption lines were also observed in the 28.6 μm cutoff wavelength AlGaAs/GaAs QWIP detector also under backillumination.[3] Response was observed at a constant level for temperatures up to 18 K above which the noise due to increased dark current became large enough to hide the response.

The intersubband transition was confirmed by measuring the polarization dependence of the photoconductivity signal showing a typical polarization response as seen in Fig. 4(a) for a wavelength of 31 μm. Similar polarization results were obtained for wavelengths of 20–32 μm. The voltage dependence of the response is shown in Fig. 4(b), which rises to a maximum and then remains relatively constant as is typical of QWIPs.

Noise was also measured using a low-noise preamplifier (SR 560) and a fast Fourier transform spectrum analyzer (SR780) with the detector at 4.2 K. The noise spectra showed no frequency dependence and had a value of $S_i=3.4\times 10^{-24}$ A^2/Hz at a bias of 145 mV. Based on this value and the peak responsivity the noise equivalent power (NEP) was found from NEP$=\sqrt{S_i}/R$ to be 4.0×10^{-12} W/$\sqrt{\text{Hz}}$ giving $D^*=6.0\times 10^9$ cm$\sqrt{\text{Hz}}$/W as a conservative estimate. The calculated spectrum without absorption gives $D^*=6.6\times 10^9$ cm$\sqrt{\text{Hz}}$/W. From the measured noise spectra and the expected dark current shot noise is given by $S_i=4qI_dg$, where q is the electron charge, I_d is the dark current, and g the optical gain obtained as $g=0.11$. This indicates a leakage current since the gain is less than that expected from QWIPs.[10] Once tunneling and defect related current is reduced the NEP and D^* should be improved.

The noise results as well as the dark currents were higher than expected. GaAs far-infrared detector samples with barriers of <20 meV (cutoff ~ 100 μm) give similar or even lower dark currents and noise values at similar temperatures.[11] The observed dark current scaled as the sample area and varied less than 5% for samples with the same area indicating that the excess current is not due to surface related leakage at the edges. The reduction of the dark current should lead to improved performance in the detectors.

In summary, the longest ($\lambda_c\sim 35$ μm) far-infrared quantum well photodetector (QWIP) which is based on bound-to-continuum intersubband transitions of GaAs/$\text{In}_x\text{Ga}_{1-x}$ As is reported. A peak responsivity of 0.45 A/W, detectivity of 6.0×10^9 cm$\sqrt{\text{Hz}}$/W, and NEP of 4.0×10^{-12} W/$\sqrt{\text{Hz}}$ from noise measurements at 4.2 K have been achieved. Detector response was observed at temperatures up to 18 K.

This work was supported in part by the NSF under Grant No. ECS-98-09746. The work at NRC was supported in part by DND. The authors acknowledge S. J. Rolfe for secondary ion mass spectroscopy measurements.

[1] B. F. Levine, J. Appl. Phys. **74**, R1 (1993).
[2] S. D. Gunapala and S. V. Bandara, ''Quantum Well IR Photodetector Focal Plane Arrays,'' in *Semiconductors and Semimetals Vol. 62*, edited by H. C. Liu and F. Capasso (Academic, San Diego, 2000), pp. 197–291.
[3] A. G. U. Perera, W. Z. Shen, S. G. Matsik, H. C. Liu, M. Buchanan, and W. J. Schaff, Appl. Phys. Lett. **72**, 1596 (1998).
[4] P. W. Pellegrini and J. R. Jimenez, ''Thin Film Epitaxial Layers on Silicon for the Detection of Infrared Signals,'' *The Physics of Thin Films Vol. 23* (Academic, San Diego, 1998), p. 115.
[5] H. C. Liu, Z. R. Wasilewski, M. Buchanan, and H. Chu, Appl. Phys. Lett. **63**, 761 (1993).
[6] O. Brafman, D. Fekete, and R. Sarfaty, Appl. Phys. Lett. **58**, 400 (1991).
[7] J. Li, H. C. Liu, M. Buchanan, Z. R. Wasilewski, and J. G. Simmons, J. Appl. Phys. **75**, 1748 (1994).
[8] K. K. Choi, *The Physics of Quantum Well Infrared Photodetectors* (World Scientific, Singapore, 1997).
[9] E. S. Koteles and W. R. Datars, Can. J. Phys. **54**, 1676 (1976).
[10] H. C. Liu, Appl. Phys. Lett. **60**, 1507 (1992).
[11] A. G. U. Perera, Opto-Electron. Rev. **7**, 153 (1999).

Downloaded 01 Feb 2001 to 131.96.4.23. Redistribution subject to AIP copyright, see http://ojps.aip.org/aplo/aplcpyrts.html.